

## ***A Variable-Speed Sensorless Drive System for Switched Reluctance Motors***

---

*Stephen J. Fedigan, Ph.D. and Charles P. Cole*

*DSPS Research and Development Center*

### **ABSTRACT**

With the advent of high-speed digital signal processors (DSPs) specialized for motion control applications, it has become possible to control motors without mechanical (speed or position) sensors. This is achieved by algorithms that estimate the desired quantities in real time, based on the electrical signals in the motor windings. Benefits include cost savings and improved reliability due to reduced component count. This application report presents a low-cost, sensorless drive system for a switched reluctance motor (SRM) based on the Texas Instruments TMS320F243 DSP. Detailed descriptions of the hardware configuration, the sensorless commutation algorithm, its implementation details, and procedures for measuring motor parameters should enable readers to rapidly duplicate and customize a sensorless SRM drive system to meet their specific application.

---

## Contents

<b>1</b>	<b>Hardware to Demonstrate Sensorless Control of the Switched Reluctance Motor Using the Texas Instruments TMS320F243 DSP</b>	<b>4</b>
1.1	Demonstration Goals	4
1.2	Hardware Description	4
1.2.1	Switched Reluctance Motor Characteristics	5
1.2.2	Digital Motor Controller	6
1.2.3	TMS320F243 Evaluation Module	7
1.2.4	Magtrol Dynamometer	7
1.2.5	Dynamometer Controller	8
1.3	Operational Procedures	8
1.4	Sensorless SRM Performance	10
<b>2</b>	<b>Control Software for a Sensorless SRM Drive System</b>	<b>11</b>
2.1	Overview of the Sensorless SRM Control Software	11
2.2	Sensorless Commutation and Velocity-Update Algorithm	13
2.2.1	Flux Estimator	14
2.2.2	Flux Estimator Implementation	15
2.2.3	Flux Reference Generator	16
2.2.4	Lockout Window	16
2.2.5	Velocity Estimator	18
2.2.6	Stall Detector	19
2.2.7	Low-Speed Operating Mode (<400 RPM)	19
2.2.8	Commutation and Velocity-Update Algorithm Summary	20
2.3	Velocity Loop	22
2.3.1	Motor Start-up Under Load	22
2.4	Current Control Loop	23
2.5	Ramp Controller	24
2.6	Serial Comms	26
<b>3</b>	<b>Calibration for a Sensorless SRM Drive System</b>	<b>27</b>
3.1	Stator Flux Estimation	27
3.2	Measuring the Voltage “Loss” Function	28
3.3	Generating a Voltage “Loss” Look-up Table	29
3.4	Measuring the Voltage “Loss” Data	29
3.5	Flux Measurement Method	30
3.5.1	Flux Measurement Hardware	31
3.5.2	Demo SRM Flux Measurements	32
3.5.3	Look-up Table Generation Method	33
	<b>References</b>	<b>34</b>

**List of Figures**

Figure 1.	Interconnection Diagram for SRM Demo Hardware .....	5
Figure 2.	SRM Power Driver Topology .....	6
Figure 3.	Software Block and Timing Diagrams .....	12
Figure 4.	Graph of Flux Estimate and Flux Threshold vs. Time .....	14
Figure 5.	SRM Power Driver Topology .....	15
Figure 6.	Flux Estimator Code .....	16
Figure 7.	Flux Estimate and Threshold at 2500 RPM Under Full Load .....	17
Figure 8.	Illustration of Sensorless Commutation Algorithm With Lockout Window .....	18
Figure 9.	Low-Speed Operating Mode With a Second Flux Threshold for an Additional Velocity Update .....	19
Figure 10.	Commutation and Velocity-Update Flow Diagram .....	21
Figure 11.	Block Diagram of the Velocity Control Loop .....	22
Figure 12.	Instantaneous Velocity Estimate and Velocity Loop Output During Start-up .....	23
Figure 13.	Block Diagram of the Current Control Loop .....	23
Figure 14.	State Transition Diagram for the Ramp Controller .....	25
Figure 15.	Flow Chart for Voltage “Loss” Measurement Program .....	28
Figure 16.	Voltage “Loss” vs. Current for the Emerson Electric SRM and the Spectrum Digital Motor Control Board .....	30
Figure 17.	SRM Magnetization Curves .....	31
Figure 18.	Analog Flux Measurement Circuit .....	32
Figure 19.	Flux Linkage Curves for Demo Platform SRM .....	33

**List of Tables**

Table 1.	Performance Parameters of the Demo SRM Drive System .....	4
Table 2.	Switched Reluctance Motor Characteristics .....	5
Table 3.	Description of Commands .....	9
Table 4.	Sensorless SRM Performance Summary .....	10
Table 5.	Execution Times of Foreground Activity .....	13
Table 6.	Serial Communications Module Commands .....	26

# 1 Hardware to Demonstrate Sensorless Control of the Switched Reluctance Motor Using the Texas Instruments TMS320F243 DSP

This section describes the hardware used to demonstrate the sensorless control of a typical switched reluctance motor (SRM) drive using the Texas Instruments TMS320F243 digital signal processor (DSP). Research completed in March of 1998 and documented in the Application Report titled "Developing an SRM Drive System Using the TMS320F240" (literature number SPRA420) led to a baseline software algorithm for conventional operation of the SRM drive using a shaft position sensor. Follow-on research completed in August of 1999 extended the performance range of a specific SRM without a shaft position sensor using a sensorless control algorithm. Detailed information on the sensorless software control algorithm can be found in Section 2. Hardware used in this follow-on research was the 3-phase, 12/8 stator-pole-configured SRM manufactured by Emerson Electric Company, and the digital motor controller board designed and manufactured by Spectrum Digital Incorporated ([www.spectrumdigital.com](http://www.spectrumdigital.com)), which utilizes the Texas Instruments TMS320F243 DSP. The hardware and software algorithm as described are intended to be used primarily for potential customer demonstrations and to serve as examples of extended performance sensorless control of SRM drive systems.

## 1.1 Demonstration Goals

The basic goals of this research work were to build upon the baseline software algorithm as described in the application report referenced above and to extend the performance range of the SRM drive using sensorless control. Performance parameters (listed in Table 1) of the SRM drive were set to cover a wide range of potential customer applications such as white goods (washing machine), compressor pumps, and blower fan applications.

**Table 1. Performance Parameters of the Demo SRM Drive System**

Speed range	150 to 4500 rpm
Load torque	no load to 48 oz-in
Speed regulation	10% over full speed/torque range

In addition to these basic requirements, other goals were to successfully start the SRM from standstill under a full load torque of 48 oz-in.

## 1.2 Hardware Description

Hardware used for this demonstration is described in the following sections. A diagram of the interconnections between the various hardware elements that make up this SRM demonstration platform is shown in Figure 1.

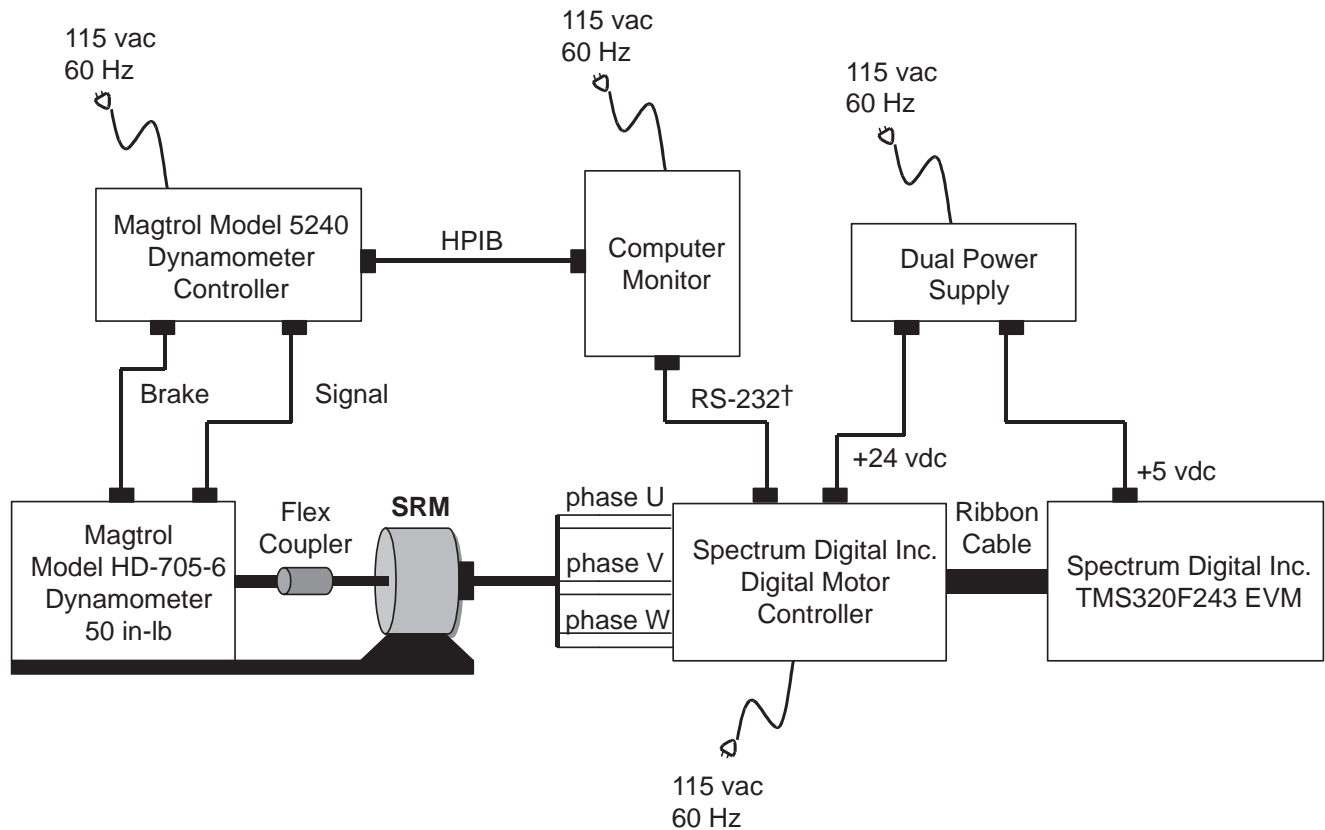


Figure 1. Interconnection Diagram for SRM Demo Hardware

### 1.2.1 Switched Reluctance Motor Characteristics

The characteristics of the switched reluctance motor are shown in Table 2.

Table 2. Switched Reluctance Motor<sup>†</sup> Characteristics

Number of phases	3
Number of stator poles	12
Number of rotor poles	8
Phase resistance	2.5 ohms
Aligned inductance	52 mH
Unaligned inductance	9.5 mH
Phase current (max)	4 amps

<sup>‡</sup> Manufactured by Emerson Electric Company for the Maytag™ Neptune™ Auto Washer.

Maytag and Neptune are trademarks of Maytag Corporation.

<sup>†</sup> TIA/EIA Standard 232-F – October 1997, Interface Between Data Terminal Equipment and Data Circuit-Terminating Equipment Employing Serial Binary Data Interchange.

## 1.2.2 Digital Motor Controller

The board is designed and manufactured by Spectrum Digital Incorporated and utilizes the Texas Instruments TMS320F243 DSP. This controller board has an ac-to-dc converter that generates a full-wave-rectified and -filtered 162-volt dc from an ac supply input of 115 vac at 50/60 Hz. With placement of on-board jumpers, the board can be configured in a voltage doubler mode to generate 320 volts dc if the intended motor application requires the higher voltage. It also has a three-phase power inverter powered from the 162-volt dc bus. This power inverter can be configured, with proper placement of jumpers, to drive typical three-phase ac induction motors, three-phase brushless dc motors, or three-phase SRMs. In the SRM configuration, the power driver uses the popular and standard two-switches-per-phase topology as shown in Figure 2.

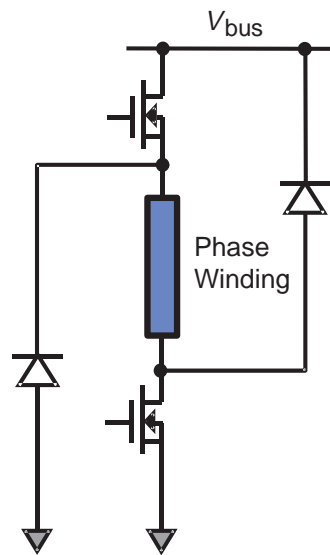


**Figure 2. SRM Power Driver Topology**

Current-sensing resistors are included in each low-side power driver leg with variable gain buffer amplifiers to output current feedback samples in each phase winding of the motor. In this example application of the SRM drive system, the gain of these buffer amplifiers has been set to give a current-sensing scale factor of 1.0 amp/volt. On-board low-voltage power supplies of +5 volts dc and +15 volts dc are also included so that this board can operate independently from 115 volts ac at 50/60 Hz.

Other features of this controller board are current-sensing resistors on the bus to enable power factor correction capability. This feature is not used in this example application. Some minor modifications to the board have been made for this example application and include removal of the R5 (0.03 ohm) bus current-sensing resistor. Current-sensing resistors R2, R3, and R4 have also been changed from 0.04 ohm to 0.2 ohm to adjust the current feedback scale factor and reduce electrical noise sensitivity. A serial communications interface (RS-232) port is also provided on the board and is used in this example application to introduce input set speed commands so that the motor speed can be changed on the fly while the motor is running.

### 1.2.3 **TMS320F243 Evaluation Module**

This evaluation module (EVM), based upon the Texas Instruments TMS320F243 digital signal processor, is designed and manufactured by Spectrum Digital Incorporated. It is an excellent platform to develop and run software on the 'F24x family of processors and was used extensively in the development and testing of the software algorithm for the sensorless control of the SRM drive system in this demonstration hardware. Key features of the TMS320F243 EVM are:

- 544 words of on-chip data memory
- 28K words of onboard memory
- on-chip FLASH memory
- on-chip UART
- MP7680 four-channel digital-to-analog converter
- 5-volt-only operation

(For additional information, see the Technical Reference on this TMS320F243 EVM published by Spectrum Digital Incorporated in 1998.)

To operate the demonstration as described in the operational procedures section, the sensorless control software must be embedded in the TMS320F243 DSP. (For details on embedding the software in FLASH, please refer to the *TMS320F20x/F24x DSP Embedded Flash Memory Technical Reference*, literature number SPRU282.)

### 1.2.4 **Magtrol Dynamometer**

The dynamometer used to control load torque on the SRM in this demonstration hardware platform is manufactured by Magtrol Incorporated. It is a load cell dynamometer (model 705-6) that features a hysteresis brake for precise torque loading up to a maximum of 50.0 in-lb of torque and has a maximum speed capability of 10,000 RPM. Power rating for the model 705-6 dynamometer is 300 watts continuous and 1400 watts for less than five minutes. To achieve the best accuracy capability of 0.25%, attention must be given to the calibration of the unit for zero offset and scale factor as specified in the user's manual. The motor shaft is attached to the dynamometer through a precision aligned flexible coupling that has been custom modified for this demonstration platform. Alignment of the motor shaft through the flexible coupling is critical to prevent vibration and mechanical induced noise at higher operation speeds above 2500 RPM. This type of flexible couplers can be obtained through Magtrol Incorporated.

### 1.2.5 Dynamometer Controller

Control of the dynamometer is provided by a Magtrol model 5240 controller that is a speed-controlled power supply, designed to interface with any type of IBM-compatible computer using an IEEE-488<sup>†</sup> general-purpose interface bus (GPIB) instrument controller. The model 5240 controller can be used to control any Magtrol Load Cell Dynamometer. In addition, it can be set to return torque-speed data to the computer when used with appropriate computer software. In this demonstration hardware, testing of the SRM performance was accomplished with an automatic-motor-testing software (M-TEST, version 2.03) provided by Magtrol.

## 1.3 Operational Procedures

To operate the demonstration, a serial communications link must be established between the 'F243 and the host PC by using a standard RS-232 through-pin serial cable. This cable is attached to the DB9 connector on the Spectrum Digital board and the COM port on the PC.

#### **WARNING:**

Do not use the DB9 connector on the EVM board. This connector is not isolated, and ignoring this warning could result in hardware damage, injury, or even death.

Commands can be issued through a terminal program such as a Hyperterm, which is included in the Windows<sup>™</sup> operating system. To properly configure Hyperterm, the connection speed must be set at 19,200 baud, with 7 data bits, odd parity, and 1 stop bit, and all flow control must be disabled.

With the connection established, the demonstration rig can be turned on, using the following procedure:

1. Power up the PC, load controller, and dynamometer brake.
2. Run the terminal program and the Magtrol M-TEST software.
3. Turn on the dual power supply.
4. Plug in the bus supply line on the Spectrum Digital board.

Once power has been applied to all of the components, the terminal program can be used to issue the 'turn on' command, which is '>' followed by a carriage return. When the EVM receives the 'turn on' command, the 'F243 injects an alignment current into phase 2. After the shaft has settled at the aligned position, the 'F243 begins commutating the motor, causing it to spool up in the counterclockwise direction to its initial target speed of 1000 RPM. At this point, the 'F243 is ready to receive new commands, which are summarized in Table 3.

Windows is a registered trademark of Microsoft Corporation.

<sup>†</sup> ANSI/IEEE Standard 488.1 – 1987, IEEE Standard Digital Interface for Programmable Instrumentation.

**Table 3. Description of Commands**

Command†	Description
>t	Turn on drive system
>sxxx	Set new target speed (in RPM) ( $0150 \leq xxx \leq 4500$ )
>b	Brake motor and reverse direction
>a	Agitate the motor
>c	Cut off the drive system

† Each command must be followed by a carriage return.

These commands can set new target speeds, reverse the motor direction, agitate, or cut off the motor. If the speed command ('>s', followed by a four-digit number between 0150 and 4500) is issued, the motor will ramp up or down at 100 RPM/sec to the new requested target speed, provided it is between 0150 and 4500 RPM. If a speed is requested above the top speed of 4500 RPM, the new target speed will be set to 4500 RPM. Likewise, if the requested target speed is below 150 RPM, the new target will be set to 150 RPM. After the ramp is completed, the software will wait for a settling period of several seconds, and then wait to receive the next speed command.

If the next command is a brake command ('>b'), the software will apply passive braking, which is accomplished by injecting a constant current into phase 2. After the motor slows down and aligns with phase 2, it will start up in the opposite direction, spool up to the initial target speed of 1000 RPM, and then continue ramping up or down to its former speed. The agitate command is quite similar to the brake command. When it is issued, the motor simulates the agitation action of a washing machine, i.e., it repeatedly brakes, aligns, reverses direction, and spools up to 1000 RPM. After repeating this sequence ten times, the software exits the agitation mode, and waits for a new command.

To turn off the motor, the user can either turn off the bus power or can issue the 'cut off' command ('>c'), which de-energizes all of the motor phases and spinlocks the processor. Once this command is issued, the user can restart the system by following the procedure outlined above. (For further details concerning the ramp controller and serial communications, please refer to Section 2.)

Note: Commands issued while the motor is ramping and settling at a new target speed will be ignored.

## 1.4 Sensorless SRM Performance

Table 4 summarizes the performance of the SRM drive system.

**Table 4. Sensorless SRM Performance Summary**

Parameter	Value/Units
Speed range	150 – 4500 rpm
Load torque	48 oz-in
Speed regulation	< 8%
– low-speed	< 8%
– mid-range	< 1%
– hi-speed	< 2%
Start-up load torque	48.0 oz-in

For operating speeds between 1000 and 3500 RPM, regulation is tighter than 1%, within the design load of 48.0 oz-in. For higher speeds, regulation is more challenging and grows to 3% at the top speed of 4500 RPM. This happens because the speed measurement resolution decreases as the speed squared, due to sample rate effects. At the low end, speed regulation is affected by the reduced frequency of speed updates. This update rate is tied to the shaft speed, and these updates occur less and less frequently as the speed is decreased. To achieve the 10% performance specification below 400 RPM, the controller enters a special low-speed operating mode, which doubles the update rate and in turn preserves the bandwidth of the velocity loop. This keeps the regulation error below 8% at 150 RPM. (For further details concerning the low-speed operating mode, please refer to Section 2.) With the help of an open-loop start-up procedure, the motor can also be started reliably under a full load of 48.0 oz-in. This is valuable in pump and compressor applications, where the load is constant throughout the entire operating speed range.

## 2 Control Software for a Sensorless SRM Drive System

This section describes the control software for a sensorless SRM drive system using the TMS320F243 DSP. The drive system is intended for demonstration purposes and is composed of a TMS320F243 evaluation module (EVM); a digital motor controller board available from Spectrum Digital Incorporated; a 3-phase, 12/8 stator-pole-configured 0.40-HP SRM manufactured by Emerson Electric Company; and a Magtrol 50.0 lb-ft dynamometer and load controller. (For further details concerning the hardware and performance specifications for this drive system, refer to Section 1.)

The control software features a flux-based sensorless algorithm for 3-phase SRMs operating on 170 V of bus voltage and up to 4.0 A of phase current. The algorithm is capable of two quadrant speed control between 150 and 4500 RPM, with better than 8% speed regulation (<1% between 1000 and 3500 RPM), and reliable start-up under a design load of 48.0 oz-in. An RS-232 serial link permits users to issue commands from a host PC to turn on, cut off, and change motor speed and the direction of rotation on the fly. This software can be launched via the EVM's JTAG port using a XDS510PP™ emulator board inline with a SPI 110 optoisolator or the software can be directly embedded in the EVM's FLASH memory. (For further details on FLASH programming, refer to the *TMS320F20x/F24x DSP Embedded FLASH Memory Technical Reference*, literature number SPRU282.)

### 2.1 Overview of the Sensorless SRM Control Software

The software for the sensorless drive system is written primarily in C, with the exception of a few assembly language subroutines for high-speed computations. The code fits into the TMS320F243's 8K of FLASH program memory and the DSP's internal RAM blocks, and requires no external memory. It consumes about 6K of program memory and 300 words of data memory. To execute the code on a TMS320C242 DSP controller, the program storage requirements can be reduced to less than 4K by replacing the look-up tables used by the commutation algorithm with polynomial interpolating functions.

As shown in Figure 3, the software is composed of five key modules: an algorithm for sensorless commutation, an outer loop for velocity control, an inner loop for current control, a serial command processor, and a ramp controller. The first three of these modules execute in the foreground. They are called from a timer interrupt service routine (ISR), which is fired every 66.7  $\mu$ sec (15.0 kHz) by a free-running onboard timer. As shown in the timing diagram of Figure 3, the commutation controller and current control loop execute every interrupt cycle (at 15.0 kHz), while the velocity loop only executes every sixth interrupt cycle (at 2.5 kHz).

XDS510PP is a trademark of Texas Instruments Incorporated.

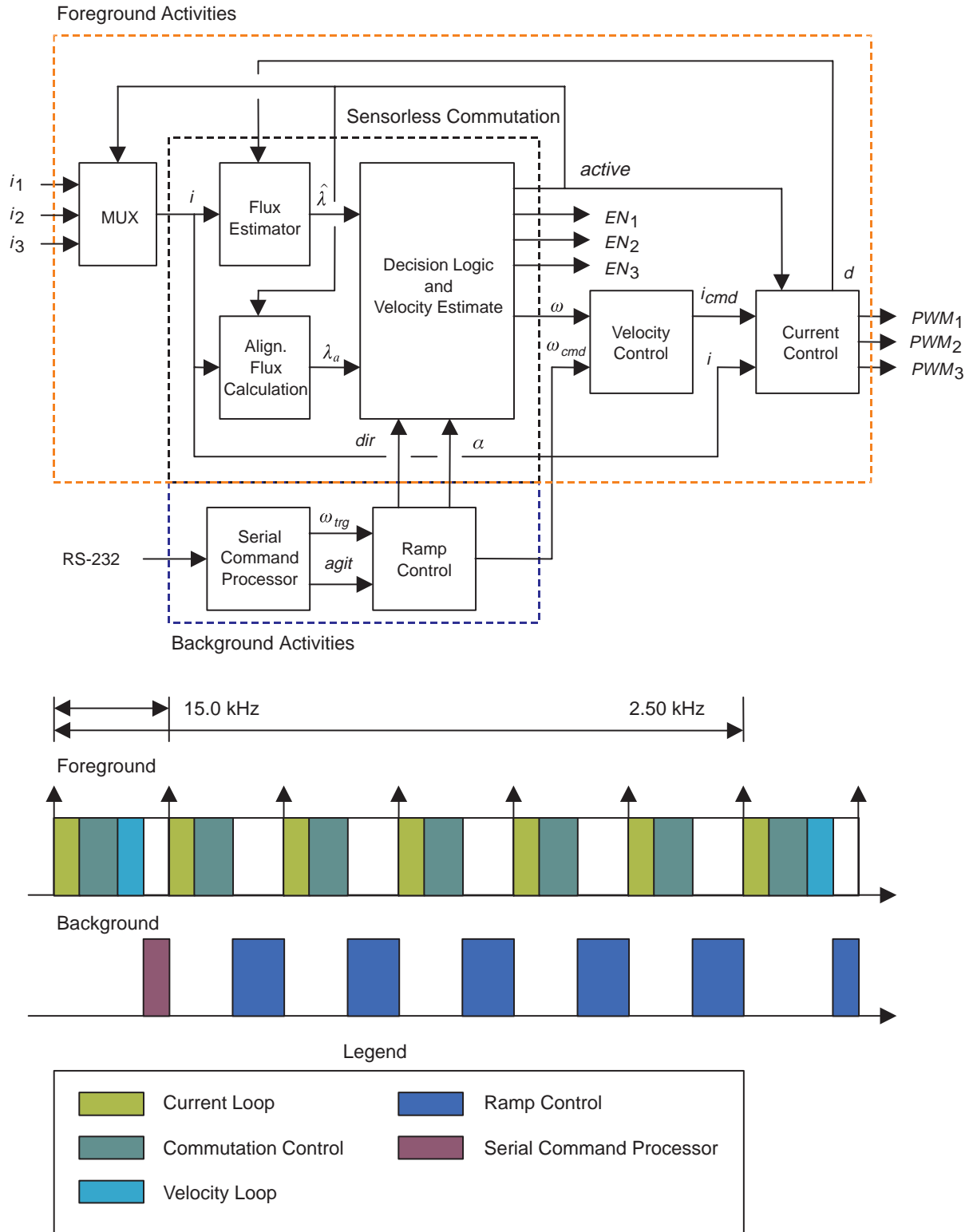


**Figure 3. Software Block and Timing Diagrams**

The execution time of each foreground activity shown in the software block diagram is listed in Table 5.

**Table 5. Execution Times of Foreground Activity**

Activity	Execution Time (μsec)
Flux Estimator	8.3
Sensorless Commutation	15.5 to 34.8
Current Control Loop	10.6
Velocity Control Loop	11.3

Note that execution time of the sensorless commutation algorithm varies. If the motor needs to switch phases and perform a velocity update, the run time will be 34.8 μsec; otherwise, the run time will be 15.5 μsec.

Overall, execution time of the ISR varies from 34.4 μsec to 53.2 μsec, depending on which activities must execute. On average, the interrupt service routine utilizes 55% of the processing time, leaving the remaining 45% for the background loop, which includes a serial command processor and ramp speed controller.

## 2.2 Sensorless Commutation and Velocity-Update Algorithm

At the core of the sensorless algorithm is the commutation controller, which contains a flux estimator, flux reference generator, and decision logic. Ideally, the decision logic should commutate the motor when the rotor and stator poles are nearly in alignment. For this particular algorithm [1], the flux in the active phase winding is compared with a reference flux, which is a scaled version of the flux at the aligned pole position. The decision logic commutates the motor when the flux linkage exceeds the switching or reference flux. To be precise, the motor is commutated when:

$$\hat{\lambda} > \alpha_c \lambda_a \tag{1}$$

where  $\hat{\lambda}$  is an estimate of flux in the active phase winding;  $\alpha_c$  is a scalar between 0 and 1, which is analogous to a conduction angle; and  $\lambda_a$  is the flux at the aligned rotor position. This commutation condition is shown graphically in Figure 4.

As indicated by condition (1), properly timed commutation depends on an accurate estimate of the flux in the active phase winding, a knowledge of the magnetization curve at the aligned rotor position, and a carefully selected firing angle.

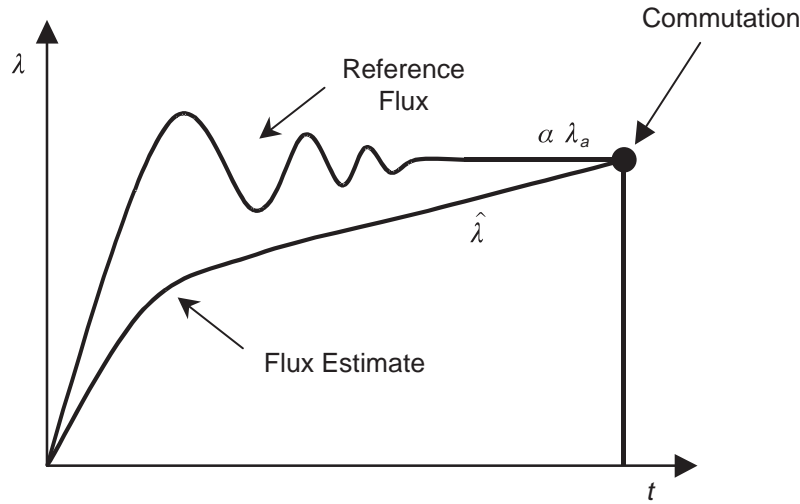


**Figure 4. Graph of Flux Estimate and Flux Threshold vs. Time**

### 2.2.1 Flux Estimator

As shown in the software block diagram of Figure 3, the quantity  $\hat{\lambda}$  is generated by the flux estimator block, which calculates flux based on the pulse width modulation (PWM) duty cycle and the current in the active phase winding. Its principle of operation is the same as a “classical” flux estimator, which uses the update law

$$\lambda_{n+1} = \lambda_n + \underbrace{v_n - i_n r_w}_{V_{EMF}} \quad (2)$$

to integrate the back EMF in the active phase winding. In Equation (2),  $v_n$  is the motor terminal voltage,  $i_n$  is the coil current, and  $r_w$  is the winding resistance. However, unlike this classical flux estimator, which requires terminal voltage *and* coil current measurements, this modified estimator only relies on current measurements. Instead of measuring the terminal voltage, it is approximated using the formula

$$v_n \approx V_{bus} d_n - v_{trans}(i_n) - v_{diode}(i_n) \quad (3)$$

which takes into account the voltage drops across the active devices in the power inverter, whose topology is shown in Figure 5. In Equation (3),  $V_{bus}$  is the bus voltage;  $d_n$ , the duty cycle;  $v_{trans}$ , the voltage drop across the power transistor; and  $v_{diode}$ , the diode voltage drop. Notice that Equation (3) assumes that the bus voltage is a stiff source, and that the  $v-i$  curves of the power devices are known. Substituting Equation (3) into the original formula, the new update law becomes

$$\lambda_{n+1} = \lambda_n + \underbrace{V_{bus} d_n - v_{trans}(i_n) - v_{diode}(i_n) - i_n r_w}_{V_{EMF}} \quad (4)$$

For simplicity, the drops across the power transistor, diode, and winding resistor are combined into a single term, called the loss voltage, permitting Equation (4) to be written as

$$\lambda_{n+1} = \lambda_n + \underbrace{V_{bus} d_n - v_{loss}(i_n)}_{V_{EMF}}, \quad \text{where} \quad v_{loss}(i_n) \equiv v_{trans}(i_n) + v_{diode}(i_n) + i_n r_w \quad (5)$$

With the “loss” voltage tabulated as a function of current, the update is performed in the software with two additions, a scalar multiplication, and a single look-up operation. (For more information on how to construct the voltage loss table, please refer to Section 3.)

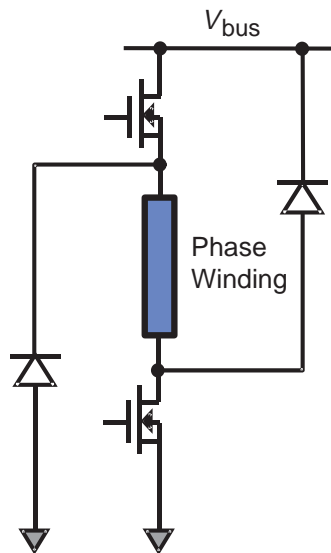


Figure 5. SRM Power Driver Topology

### 2.2.2 Flux Estimator Implementation

The subroutine `update_flux_estimate()` updates the flux estimate based on the duty cycle applied to the PWM generator and the current measured in the active phase winding. As shown in Figure 6, the code implements Equation (5) in a straightforward manner, with the exception of the look-up operation. To perform the look-up operation, an index into the 256-point table is generated by shifting  $i_n$ , a 10-bit unsigned integer, two places to the right. The address of the desired table element is formed by adding this index to the table’s base address, and the table is accessed by invoking the assembly language subroutine `long_table_read()`. This subroutine reads the desired table element from FLASH program memory using a table-read operation (`TLBR`) and returns the value in a desired data memory address. After completing the table read, both terms in Equation (5) are added to the previous flux estimate to form the new one, and the update is stored in the SRM data structure. This update is a scaled version of actual flux linkage in the winding. To convert it to physical units of V-sec, multiply by the following scale factor:

$$\hat{\lambda} = \frac{\text{anSRM} \rightarrow \text{fluxEstimate}}{1000 \times 15000} \quad (6)$$

In Equation (6), the factor of 1000 reflects the fact that the actual volts have been scaled by the maximum duty cycle count of 1000, and the factor of 15,000 reflects the fact that the time-step of 66.7  $\mu\text{sec}$  has been omitted from the integration.

```

void update_flux_estimate(anSRM_struct *anSRM)
{
    int phase;
    long temp1, temp2;
    long dflux;

    phase = anSRM->Active;

    /*-----*/
    /* update flux linkage estimate */
    /*-----*/
    temp1 = (VBUS * anSRM->dutyRatio[phase]);
    long_table_read(VoltTable+(anSRM->iFB[phase]>>2), &temp2);
    dflux = (temp1-temp2);

    anSRM->fluxEstimate[phase] = anSRM->fluxEstimate[phase] + dflux;

    if (anSRM->fluxEstimate[phase] < 0 ) {
        anSRM->fluxEstimate[phase] = 0;
    }
}

```

**Figure 6. Flux Estimator Code**

### 2.2.3 Flux Reference Generator

To check the commutation condition, the decision logic must compare the flux estimate against a reference flux  $\lambda_c$ , which is the product of a conduction angle  $\alpha_c$  and the flux at the aligned rotor position  $\lambda_a$ . The conduction angle  $\alpha_c$  is established by the ramp controller, which varies  $\alpha_c$  as a function of operating speed to maximize the motor's efficiency. The quantity  $\lambda_a$ , is returned by the subroutine `get_alignedFlux()`. This routine looks up what the flux would be at the aligned rotor position, given the current  $i_n$  and the active phase winding. As in Section 2.2.2, the `long_table_read()` subroutine must be invoked to retrieve the desired table element from FLASH memory.

### 2.2.4 Lockout Window

The decision logic which has been described to this point will time the commutations properly if the motor has been well characterized and if a *low-noise* current measurement is available. However, under certain operating conditions, noise levels in the current signal will rise, and this may trip the decision logic at the wrong moment. While the integral action of the flux estimator naturally filters out noise, the flux threshold is more sensitive, since it depends only on the *instantaneous* current. At low current levels, present at the beginning of the commutation cycle, the noise may be sufficient to suddenly drop the switching threshold, and accidentally trip the commutation logic. This problem is particularly apparent at high load torques and manifests itself in the form of motor speed oscillations, which are shown in Figure 7.

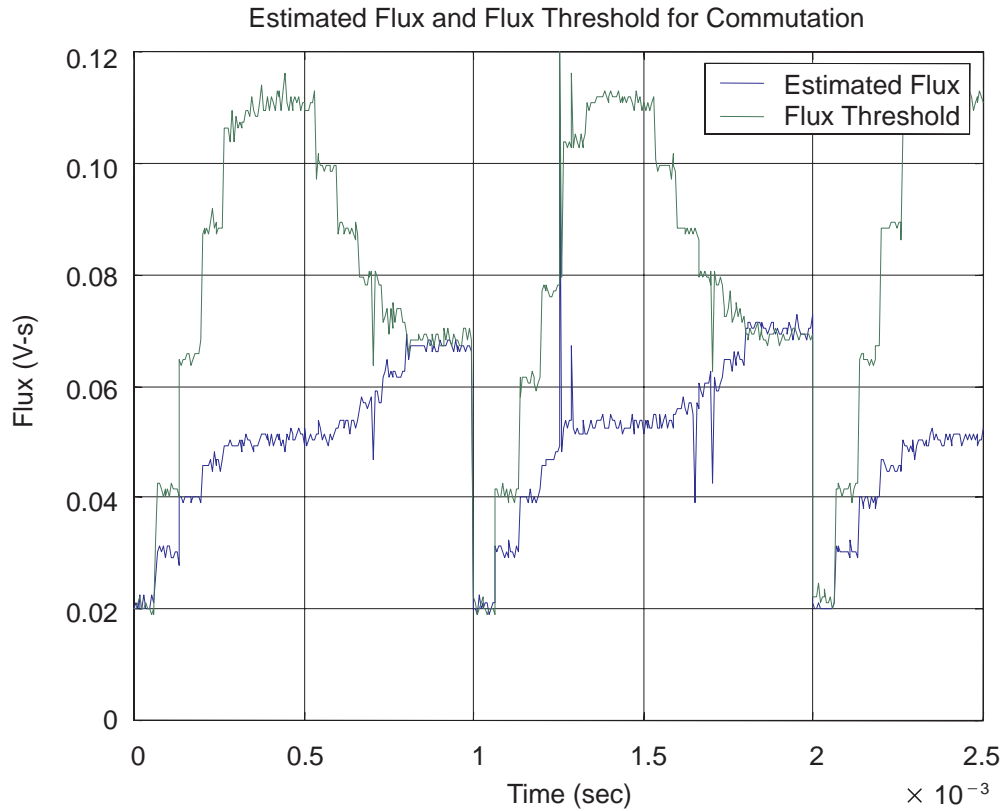


**Figure 7. Flux Estimate and Threshold at 2500 RPM Under Full Load. The flux threshold comes perilously close to tripping the commutation logic at the beginning of the commutation cycle.**

By enforcing a lockout window, depicted in Figure 8, which prohibits commutation for three sample periods (200  $\mu$ sec at 15.0 kHz) at the beginning of the commutation cycle, current noise is unable to prematurely trip the commutation logic. While improving the noise rejection of the commutation algorithm, this lockout interval does impose an upper limit on the motor's commutation rate, which in turn, limits the motor's maximum speed to 12,500 RPM.

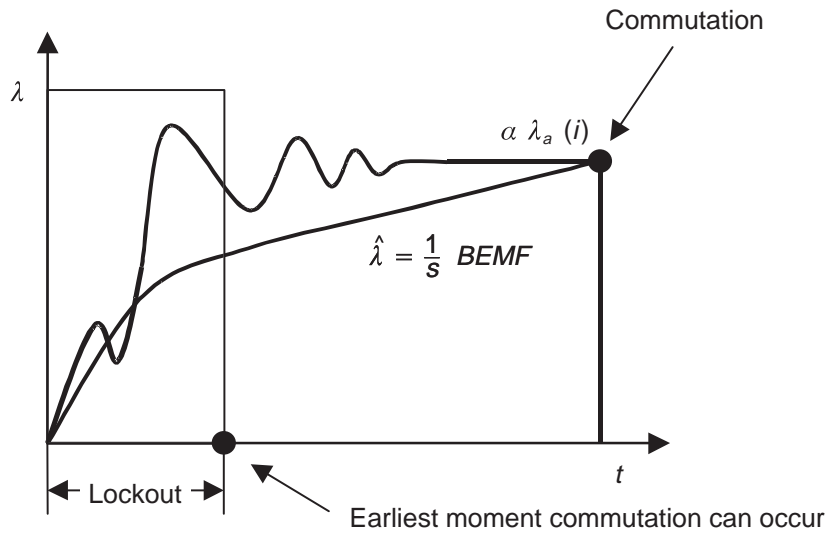


**Figure 8. Illustration of Sensorless Commutation Algorithm With Lockout Window**

### 2.2.5 Velocity Estimator

To estimate shaft velocity, a software timer counts the number of sample periods between successive commutations. When a commutation occurs, the instantaneous velocity is evaluated in RPM using the formula

$$\hat{\omega}_{INST} = K_{conv} \left( \frac{\Delta\theta}{\Delta t} \right) = K_{conv} f_s \left( \frac{\Delta\theta}{N} \right) = \frac{37,500}{N} \quad (7)$$

where  $N$  is the sample count,  $K_{conv}$  converts rads/sec to RPM, and  $f_s$  is the sampling frequency of 15.0 kHz. Since Equation (7) involves a reciprocal calculation, this formula is implemented as an assembly language function. This function performs the reciprocal operation using 16 back-to-back conditional subtract instructions (SUBC). As a result, the entire operation only requires 2.0  $\mu$ sec.

After the instantaneous velocity is calculated, the estimate is processed by a first-order infinite impulse response (IIR) filter of the form

$$\hat{\omega}_{FILT_{n+1}} = \beta \hat{\omega}_{FILT_n} + (1 - \beta) \hat{\omega}_{INST} \quad (8)$$

where  $\beta$  is a number close to 1.0 before it is passed on the velocity loop. This additional filtering deliberately reduces the velocity loop bandwidth to prevent the velocity loop from acting on noisy estimates. This filter block also improves operation at high speeds where the instantaneous velocity can vary significantly from estimate to estimate due to the small number of samples in a commutation period. By providing the velocity loop with a velocity measurement “averaged” over many commutation periods, speed oscillations are avoided.

## 2.2.6 Stall Detector

If the instantaneous shaft velocity drops below 60 RPM after the motor startup has completed, a stall detector in the decision logic will engage. After the logic detects a stalled condition, it calls a subroutine which immediately cuts off the motor. This routine sets all PWM generator duty cycles to zero, switches off the lowside power transistors, zeroes out all of the desired currents, illuminates all LEDs on the EVM board, and goes into an infinite loop. A processor reset is required to restart the system. This safety feature prevents the motor from overheating if the shaft suddenly becomes locked in place.

## 2.2.7 Low-Speed Operating Mode (<400 RPM)

As the shaft speed is lowered, velocity updates arrive with decreasing frequency, and the bandwidth of the velocity loop suffers. If the motor is suddenly loaded at a low operating speed (<400 RPM), the integrator in the velocity loop may not respond before the shaft velocity dips low enough to trigger the stall detector. To help improve loop bandwidth under these conditions, at speeds below 400 RPM, the commutation algorithm enters a special low-speed operating mode. In this mode, the velocity-update rate is doubled, by estimating the velocity twice every commutation cycle. As shown in Figure 9, this is done by adding a second flux threshold, which triggers *only* a velocity update.

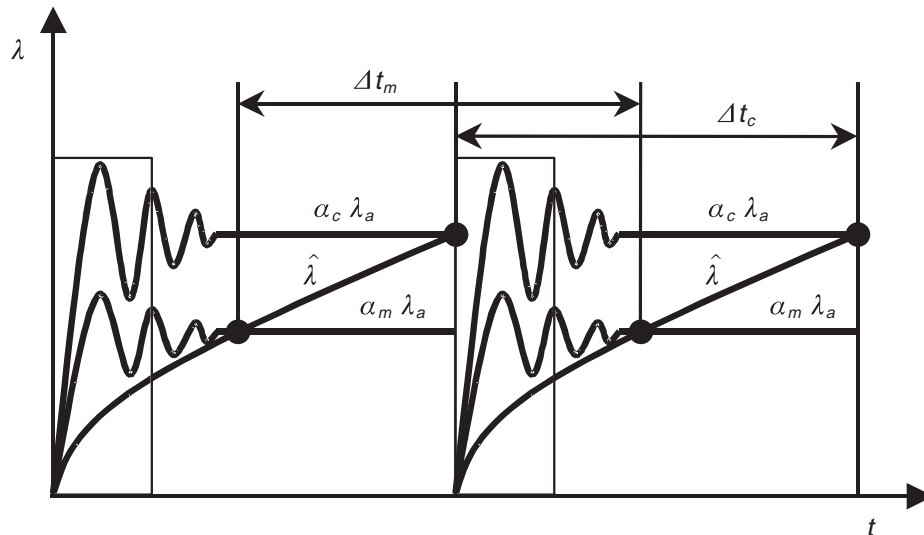


**Figure 9. Low-Speed Operating Mode With a Second Flux Threshold for an Additional Velocity Update**

As before, this threshold is a scaled version of the aligned rotor flux. Due to the sawtooth shape of the flux waveform, by setting  $\alpha_m = \alpha_c / 2$ , the new velocity update will occur approximately midway through the commutation. To implement the midway velocity update, a second counter is used to keep track of the number of samples between successive crossings. These overlapping measurement intervals permit the update rate to be doubled, and using this approach, it has been possible to extend the lower speed range from 300 RPM to 150 RPM. As in the commutation, a lockout interval is enforced to prevent current noise from accidentally triggering a velocity update at an unintended moment.

## 2.2.8 Commutation and Velocity-Update Algorithm Summary

The flowchart in Figure 10 summarizes the entire commutation and velocity-update algorithm. After the algorithm commutates the motor, it resets the flux estimator, the lockout sample counter, and the second velocity counter. Every sample period, the ISR calls the sensorless commutation routine, which increments both velocity counters. If the lockout counter is non-zero, it is decremented just before exiting the subroutine. However, if the lockout counter has expired, a commutation can occur, and further tests are performed. If low-speed mode is enabled (<400 RPM) and the first velocity update has not occurred, the flux estimate is compared against the first threshold. If the estimate has crossed the threshold, a new instantaneous velocity is calculated using the value in the first update counter, and a flag is set to indicate that the first update has occurred. This flag is important, because if it is not used, then the velocity update will occur every time the ISR is invoked until the commutation cycle ends, each time with a velocity estimate of 12,500 RPM! Following the first threshold crossing, the algorithm will check the flux estimate against the second flux threshold. When the second threshold is crossed, the velocity is updated using the second counter, and the motor is commutated.

When the motor is commutated, the current request for the active winding is zeroed, and the software advances to the next active phase, based on the direction of rotation. Next, the velocity loop's output is assigned to the current request for the next active winding. While this assignment will be made the next time the velocity loop is executed, it may take up to six sample periods for this to happen. While a variable delay of one to six sample periods is acceptable at low operating speeds, this causes problems at high speeds where there is a much smaller number of samples in a commutation cycle. Finally, the A/D MUX is switched to the next channel, and the lowside insulated gate bipolar transistor (IGBT) is turned on for the next phase winding and the lowside IGBT in the previous phase is turned off.

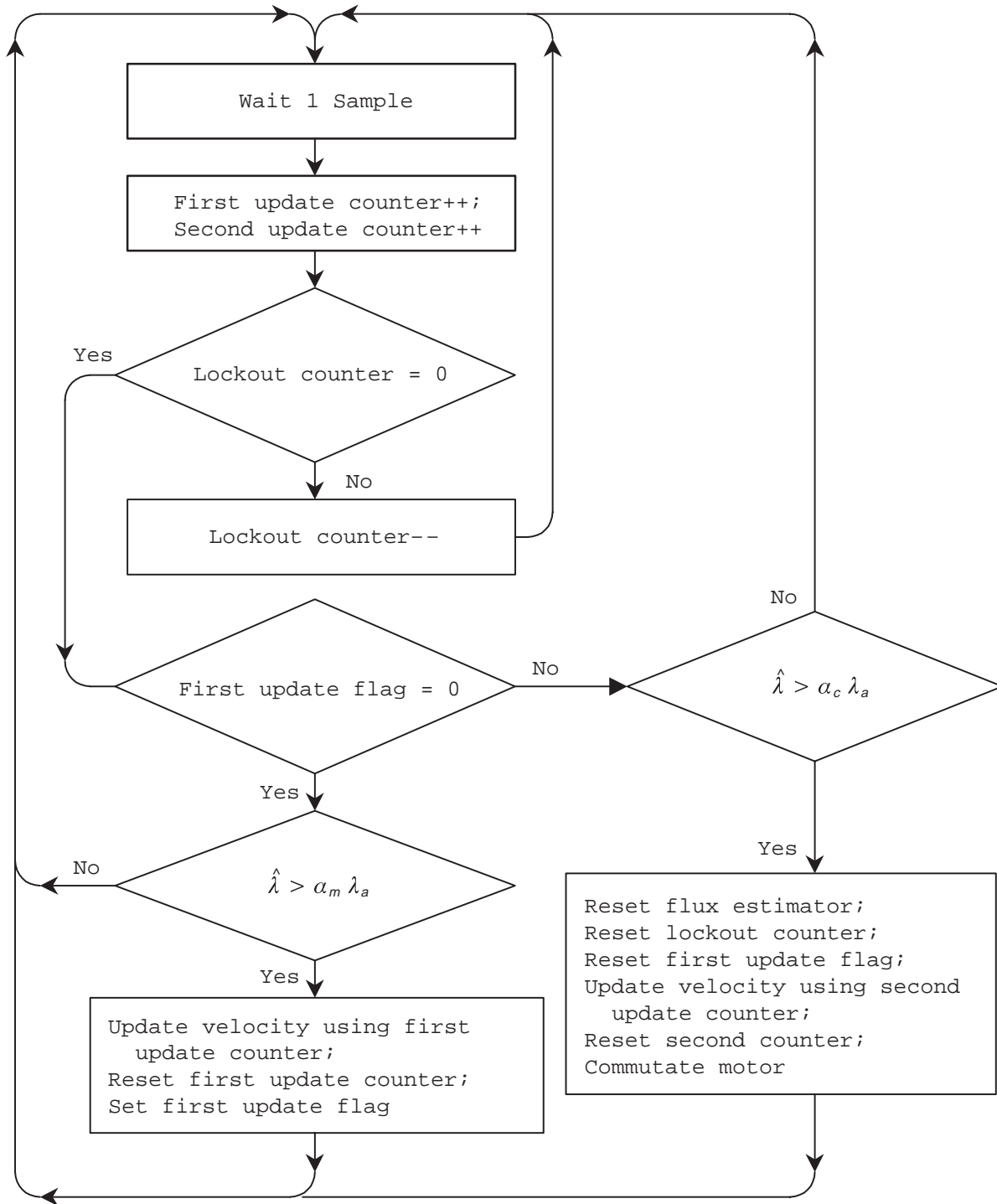


Figure 10. Commutation and Velocity-Update Flow Diagram

## 2.3 Velocity Loop

The velocity loop, which executes at a frequency of 2.50 kHz, employs a discretized proportional-integral (PI) control law to control motor shaft speed. The proportional term in the control law damps out speed oscillations and the integral term drives the DC speed errors to zero. As shown in the block diagram of Figure 11, for safety reasons, a windup limit of 6.25 A in the positive direction and the same in the negative direction is imposed on the integrator. In addition, an upper and a lower current command limit are placed on the output of the velocity loop. The upper limit is imposed for safety reasons and varies with operating speed; the lower positive limit ensures that there is sufficient amount of current to make commutation decisions.

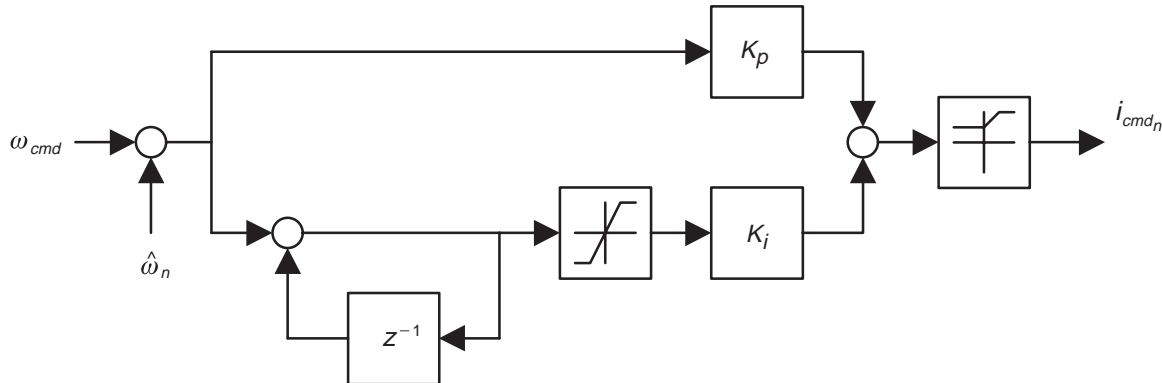
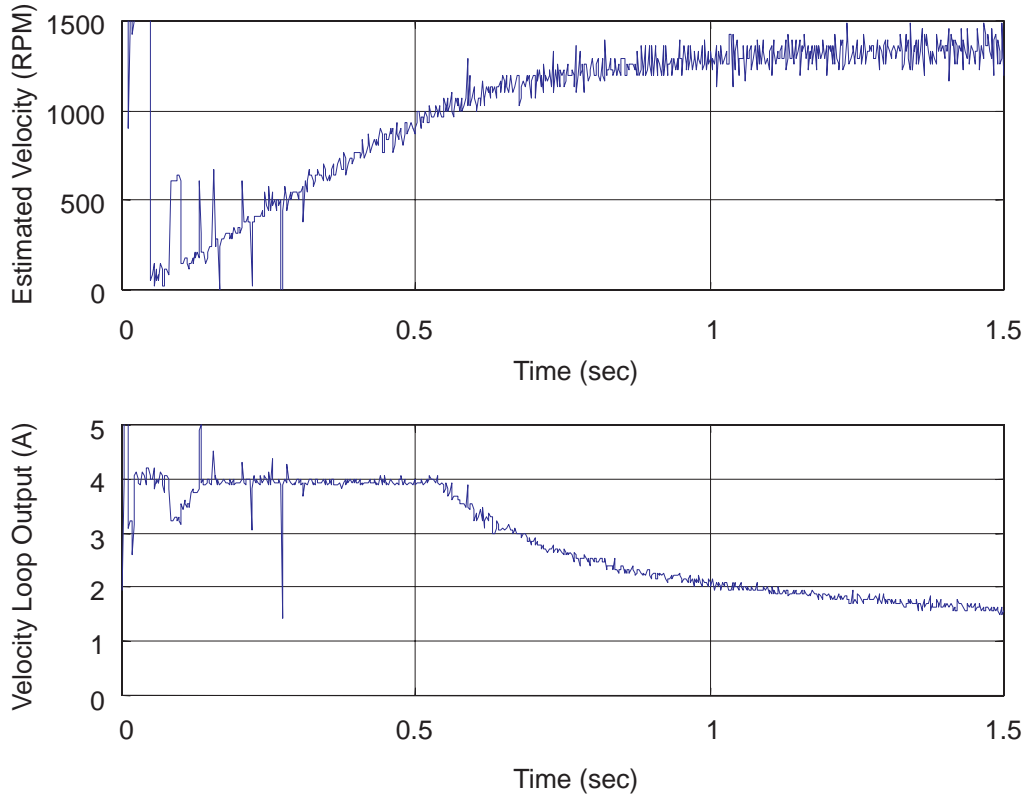


Figure 11. Block Diagram of the Velocity Control Loop

### 2.3.1 Motor Start-up Under Load

When the motor is started under load, the software counters that gauge the time between commutations can roll over, corrupting the speed estimates, and causing the velocity loop to command an improper amount of current. When this happens, the motor may experience start-up hesitation, may start up in the wrong direction, or may even stall altogether. To solve this problem, the integrator in the velocity loop is given a large initial value, which exceeds the current command limit. This causes the initial velocity estimates to be neglected and a large amount of torque to be applied to the motor. In effect, the velocity controller runs open-loop. When the velocity estimates start to exceed the initial target velocity of 1000 RPM, the integrator begins “unwinding” at a rate that depends on the difference between the estimated and desired velocity. As the integrator output decreases, eventually the velocity loop output falls below the current command limit, and the velocity controller resumes closed-loop operation and regulates the speed to 1000 RPM.

This initial integrator value should be sufficient to start the motor up reliably under full load, but should be no larger than necessary. A oversized value will cause too much velocity overshoot, perhaps more than the application can tolerate, whereas an undersized value may not start the motor up reliably. In the code, an initial integrator value has been chosen which is sufficient to start the motor up reliably under a load of 48.0 oz-in. The start-up procedure which has been described is shown in Figure 12, which graphs the estimated velocity and the command current versus time for a no-load condition.



**Figure 12. Instantaneous Velocity Estimate and Velocity Loop Output During Start-up**

In Figure 12, it is evident that the velocity is overestimated immediately following start-up. This causes a momentary drop in the integrator output from saturation, but the integrator winds up again, the velocity controller saturates for approximately the first 0.50 seconds. Shortly after reaching the initial target velocity, the integrator unwinds enough to bring the velocity controller out of saturation, and the system resumes closed-loop operation. The velocity loop overshoots about 30% under no-load conditions, but under the design load of 48.0 oz-in, the overshoot is less than 10%.

## 2.4 Current Control Loop

The current control loop, illustrated in Figure 13, which executes at the sampling frequency of 15.0 kHz, employs a proportional control law to realize the current requests which arrive from the velocity loop.

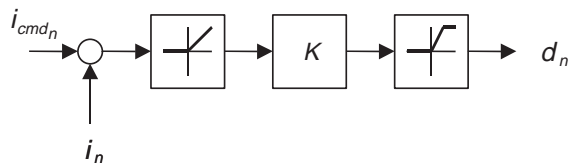


**Figure 13. Block Diagram of the Current Control Loop**

Every sample period, the current controller reads the latest current sample and calculates the current error, which is the difference between the measured and requested current. For positive errors, the controller calculates a duty cycle to the active PWM channel in proportion to the error. This calculated duty cycle becomes the applied one, provided that the calculated value is below the current command limit. Otherwise, the assigned duty cycle is the saturation limit. This saturation limit is set to 50% for start-up, but is relaxed to 90% after the motor reaches its steady-state operating speed. A 100% duty cycle is never permitted, because the drivers need time to refresh. For negative errors, the duty cycle is set to zero; this soft-chops the channel, and the current decays until the error once again becomes positive.

## 2.5 Ramp Controller

The ramp controller receives speed and direction commands from the serial comms module and applies the necessary sequence of commands to the commutation controller, velocity loop, and current loop to achieve the new target speed and direction. It runs in the background as a software-state machine. After the motor has settled to a new target speed and direction, the ramp controller enters its wait state. In this state, it continually checks with the serial command processor to see if a new command has arrived across the RS-232 link.

If a new target speed arrives, the ramp controller shifts into its ramp state, as shown in the state transition diagram of Figure 14. Depending upon whether the new target speed is above or below the current operating speed, the ramp controller will either increment or decrement the current command speed by 1 RPM. As the command speed is increased or decreased, the conduction angle is adjusted for efficient torque production and the current command limit is also adjusted. If the command speed falls below 400 RPM, the low-speed operating mode is activated, which doubles the velocity-update rate. A real-time delay is also inserted, to ensure specific ramp-up and ramp-down rates of 100 RPM/sec or 50 RPM/sec, respectively. The ramp controller remains in this state until the command speed has reached the target speed. When this happens, the controller resets the settle counter and transitions into the settle state. The purpose of this state is to allow any speed transients to die down before accepting any new target speeds from the serial command processor. The controller remains in the settle state until the counter expires, which happens after approximately two seconds. When the counter expires, the controller returns to the wait state, and awaits a new target speed.

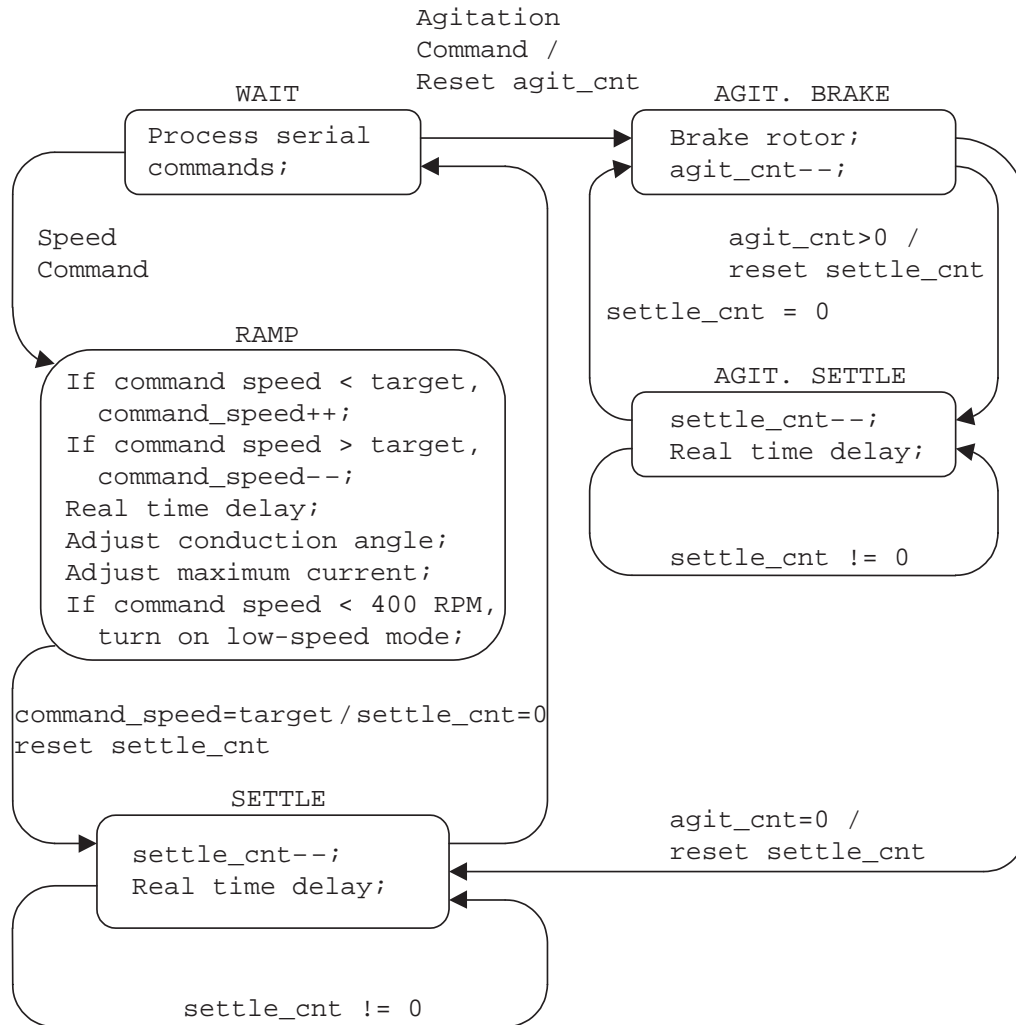


**Figure 14. State Transition Diagram for the Ramp Controller**

If the controller receives an agitation command, it resets its agitation counter before moving into the agitation brake state. Once there, a braking routine is called, disables the velocity loop and commutation controller. To passively brake the motor, phase 2 of 2 is energized with a constant current command of 3.0 A. The software delays four seconds while the motor brakes and the shaft aligns. Next, the phase is de-energized, the motor data structure, various counters and flags are re-initialized, and a new target speed of 1000 RPM is established and the commutation direction is reversed. To restart the motor, phase 0 or 1 is energized, depending on the direction of rotation, the A/D MUX is switched to the appropriate channel, and the commutation and velocity loops are re-enabled. Once the motor has started in the opposite direction, the agitation counter is decremented, the settle counter is reset, and the ramp controller enters the agitation settle state. It remains in this state for about 20 seconds, which allows the motor to settle to its 1000-RPM target speed. After the settle counter expires, the processor repeats until the agitation counter reaches zero, at which point, the controller transitions to the settle state, and eventually to the wait state, ready to accept a new serial command.

## 2.6 Serial Comms

The serial communications module receives and processes character command strings which are sent by users across the RS-232 link from the host computer. The serial communications interface (SCI) on the 'F24X is configured to run at 19,200 baud with 7 data bits, 1 stop bit, and odd parity. The communications module has five commands in its command set, which are summarized in Table 6.

**Table 6. Serial Communications Module Commands**

Command†	Description
>t	Turn on drive system
>sxxxx	Set new target speed (in RPM) (0150 ≤ xxxx ≤ 4500)
>b	Brake motor and reverse direction
>a	Agitate the motor
>c	Cut off the drive system

† Each command must be followed by a carriage return.

These commands are used to turn on the drive system, set a new target speed, reverse motor direction, agitate the motor, and cut off the drive. Note that all commands start with a '>' lead-in character, followed by a command character, and must end with a carriage return, which is not shown in the command column. The speed command 's' character is followed by four digits and a carriage return to indicate a new target speed.

The command processor is implemented as a software-state machine, and is invoked only when the ramp controller is in the wait state. (The exception to this is the 'turn on' command, which must be issued to initiate the motor start-up sequence.) Commands which are issued at other times, such as when the ramp controller is ramping the motor to a new target speed, are ignored. When the command processor is called, it checks to see if a character is waiting in the SCI receive buffer. If a character has arrived, that character is processed; otherwise, the routine promptly exits and returns control to the ramp controller. The action which is taken depends on the newly received character and the current state of the command processor.

In its default lead-in state, the command processor waits for a lead-in character. Once a lead-in character is received, the processor transitions to the command state. In this state, it waits for a valid command character. If the 'turn on' command 't' is received, the command processor waits for a carriage return, and then sets the 'turn on' flag. This begins the motor startup sequence. If the speed command character 's' is received, the processor waits for four digits, converts these four characters to a number, and then waits for a carriage return. At this point, the processor checks to see if the target speed is within bounds. If not, the processor limits the upper speed to 4500 RPM and the lower speed to 150 RPM. Next, the processor notifies the ramp controller that a new target speed has arrived by setting a flag and then returns to the lead-in state. If the agitation command 'a' is received, the agitation counter is reset, the ramp controller is placed in the agitation brake state (starting the agitation motion sequence), and the processor returns to the lead-in state. If the reverse command 'b' is received, the processor goes through passive breaking and alignment, starts the motor in the opposite direction, places the ramp controller in the ramp state to bring the motor up to its previous speed. This is the same sequence as a single agitation. If the 'cut off' command 'c' is received, the processor disables all interrupts, cuts off the motor in the same manner as the stall detector, and returns to the lead-in state.

### 3 Calibration for a Sensorless SRM Drive System

The sensorless algorithm presented in Section 2 depends on an accurate estimation of flux in the active phase winding. To enhance estimation accuracy, this algorithm includes the voltage drops across the power devices, which must be obtained as a function of current. The first part of Section 3 describes a technique for measuring the combined voltage drop across the power devices and the winding resistance as a function of current using the existing demonstration hardware. Besides an accurate flux estimate, the algorithm requires a knowledge of the magnetization curve at the aligned rotor position. The second part of Section 3 documents an analog flux-measuring circuit used to obtain the aligned magnetization curve to a high degree of accuracy. With this procedure, users can adapt the sensorless algorithm for SRMs with different electrical properties.

#### 3.1 Stator Flux Estimation

Besides a knowledge of the magnetization curves at the aligned rotor position, an accurate flux estimate must be developed by the motor-control software to successfully commutate the motor. To estimate the flux linkage, the back EMF of the active phase winding is integrated, using the update law:

$$\lambda_{n+1} = \lambda_n + \underbrace{v_n - i_n r_w}_{V_{EMF}} \quad (9)$$

In Equation (9),  $v_n$  is the motor terminal voltage,  $i_n$  is the coil current, and  $r_w$  is winding resistance. To reduce the cost of the motor drive system, the terminal voltage is not measured explicitly. Instead, it is approximated, using the formula

$$v_n \approx V_{bus} d_n - v_{trans}(i_n) - v_{diode}(i_n) \quad (10)$$

where  $V_{bus}$  is the bus voltage;  $d_n$ , the duty cycle;  $v_{trans}$ , the voltage drop across the power transistor; and  $v_{diode}$ , the diode voltage drop. Notice that Equation (10) assumes that the bus voltage is a stiff source, and that the  $v-i$  curves of the power devices are known. Substituting Equation (10) into the original formula, the new update law becomes

$$\lambda_{n+1} = \lambda_n + \underbrace{V_{bus} d_n - v_{trans}(i_n) - v_{diode}(i_n) - i_n r_w}_{V_{EMF}} \quad (11)$$

For simplicity, the drops across the power transistor, diode, and winding resistor are combined into a single term, called the loss voltage, permitting Equation (11) to be written as

$$\lambda_{n+1} = \lambda_n + \underbrace{V_{bus} d_n - v_{loss}(i_n)}_{V_{EMF}}, \quad \text{where} \quad v_{loss}(i_n) \equiv v_{trans}(i_n) + v_{diode}(i_n) + i_n r_w \quad (12)$$

In Equation (12), the update is performed in the software with two additions, a scalar multiplication, and a single look-up operation.

### 3.2 Measuring the Voltage “Loss” Function

To implement Equation (12), the “loss” voltage is measured as a function of current and a look-up table is constructed. This is accomplished by applying a fixed duty cycle PWM waveform to the motor winding. After the transients die down, the flux on the left- and right-hand side of Equation (12) will be equal, and can be cancelled out, leaving the steady-state equation:

$$v_{\text{loss}}(i_n) = V_{\text{bus}} d_n \quad (13)$$

A simple program, whose flow diagram is shown in Figure 15, can be written on the 'F243 automate data collection for the look-up table construction. The program begins by setting up the PWM generator and clearing the index counter. At the start of the program loop, the compare register is assigned the index value, which generates a fixed PWM duty cycle corresponding to  $d_n = n/n_{\text{max}}$ , where  $n_{\text{max}}$  is the counter value that corresponds to a 100% duty cycle. For a 'F243 running at 20.0 MHz with a carrier frequency of 20.0 kHz,  $n_{\text{max}} = 1000$ . After applying the fixed duty cycle, the program waits for several seconds until the current reaches a steady-state value. When this happens, the current-voltage pair is recorded in an array. Next, the index is advanced, and if the new index value is less than  $n_{\text{final}}$ , the process is repeated.

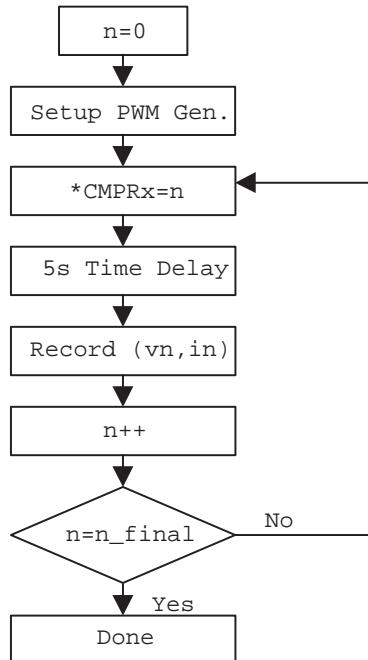


Figure 15. Flow Chart for Voltage “Loss” Measurement Program

To avoid blowing fuses that are located on the digital motor controller board or damaging components,  $n_{\text{final}}$  must be carefully chosen. To calculate an approximate value for  $n_{\text{final}}$ , calculate the “loss” voltage at the maximum current, using the formula:

$$V_{\text{loss}}(i_{\text{max}}) = V_{\text{diode}}(i_{\text{max}}) + V_{\text{trans}}(i_{\text{max}}) + i_{\text{max}} r_w \quad (14)$$

From this, calculate the duty cycle needed to generate this “loss” voltage:

$$n_{\text{final}} = \left\{ \frac{V_{\text{loss}}(i_{\text{max}})}{V_{\text{bus}}} \right\} n_{\text{max}} \quad (15)$$

Using an  $i_{\text{max}} = 4.0$  A, a diode drop of 0.70 V, and a voltage drop of 1.1 V across the IGBT, a winding resistance of 2.5 ohms, a typical bus voltage of 170.0 V, and an  $n_{\text{max}} = 1000$ ,  $n_{\text{final}} \approx 70$ .

### 3.3 Generating a Voltage “Loss” Look-up Table

After the voltage-current data is recorded in the array, it is exported via the XDS510™ to the PC, the data is fitted with a polynomial curve, with voltage as a function of current. To simplify calculation of the table index, the function is evaluated at the current points

$$i_n = i_{\text{max}} \left( \frac{n}{256} \right) \quad \forall n = 0 \dots 255 \quad (16)$$

Using these points, an index into the 256-point look-up table can be rapidly calculated by right-shifting the 10-bit current measurement over two places.

### 3.4 Measuring the Voltage “Loss” Data

Figure 16 shows a loss table constructed exactly in the manner described in the preceding section. This figure contains two curves, which compare the total  $v_{\text{loss}}$  against purely ohmic losses. At low currents, the voltage drops across the diode and the transistor dominate; whereas, at higher currents, this drop becomes almost a constant 1.8 volts, and the ohmic losses dominate. As the figure shows, accounting for the active components significantly improves the accuracy of the flux estimator, particularly at low currents, where the voltage losses are due primarily to the high dynamic impedance of the diode and the transistor. By including the power devices, motor commutation is improved considerably under no-load and light-loading conditions, resulting in more accurate speed regulation.

XDS510 is a trademark of Texas Instruments Incorporated.

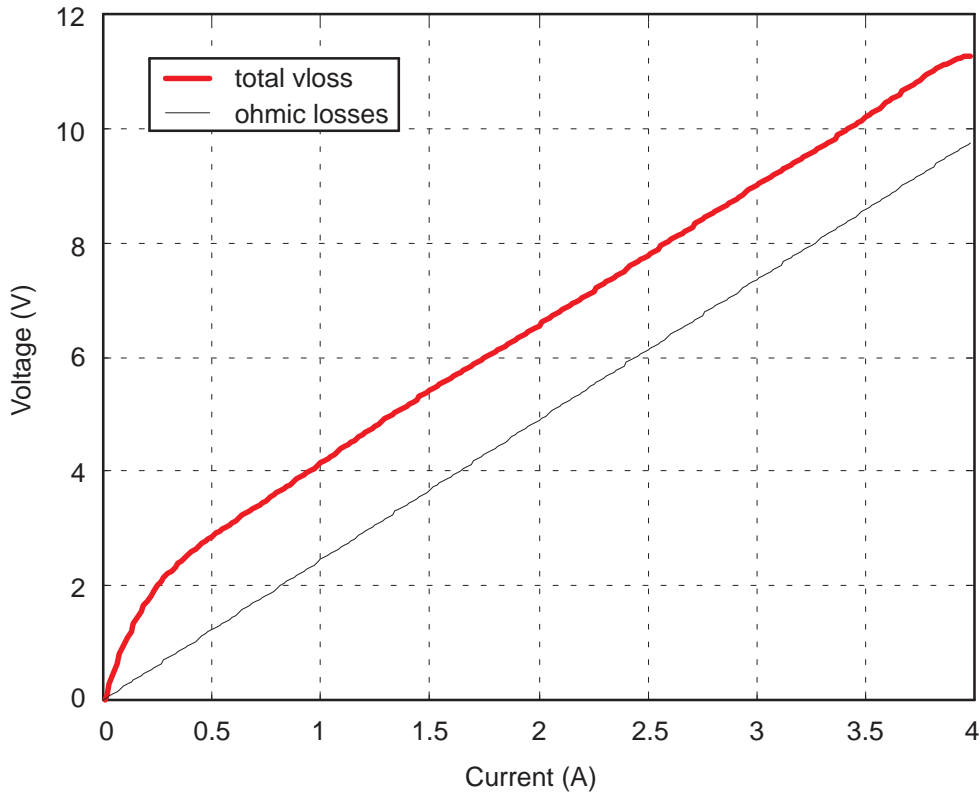


**Figure 16. Voltage “Loss” vs. Current for the Emerson Electric SRM and the Spectrum Digital Motor Control Board**

### 3.5 Flux Measurement Method

In most sensorless commutation methods, it is very desirable to have a full set of SRM magnetization curves (as in Figure 17) showing typical flux linkage (V-sec) versus phase current (amps) over the full angular range from unaligned to fully aligned rotor position. These flux linkage measurements require a precision angle indexer to hold the SRM shaft while making the measurement of flux linkage versus current flowing through the motor phase winding. This SRM magnetic model is then used along with an estimate of the flux linked by a phase to determine rotor position. The commutation algorithm used in the SRM demonstration platform only requires the flux linkage characteristic at the aligned rotor angle. Since injecting a DC current into the phase winding causes the rotor poles to align with the stator, no special alignment hardware is required. After the rotor shaft settles into alignment with the stator, flux data is then taken at this aligned rotor position using the flux measurement hardware as described in Section 3.5.1.

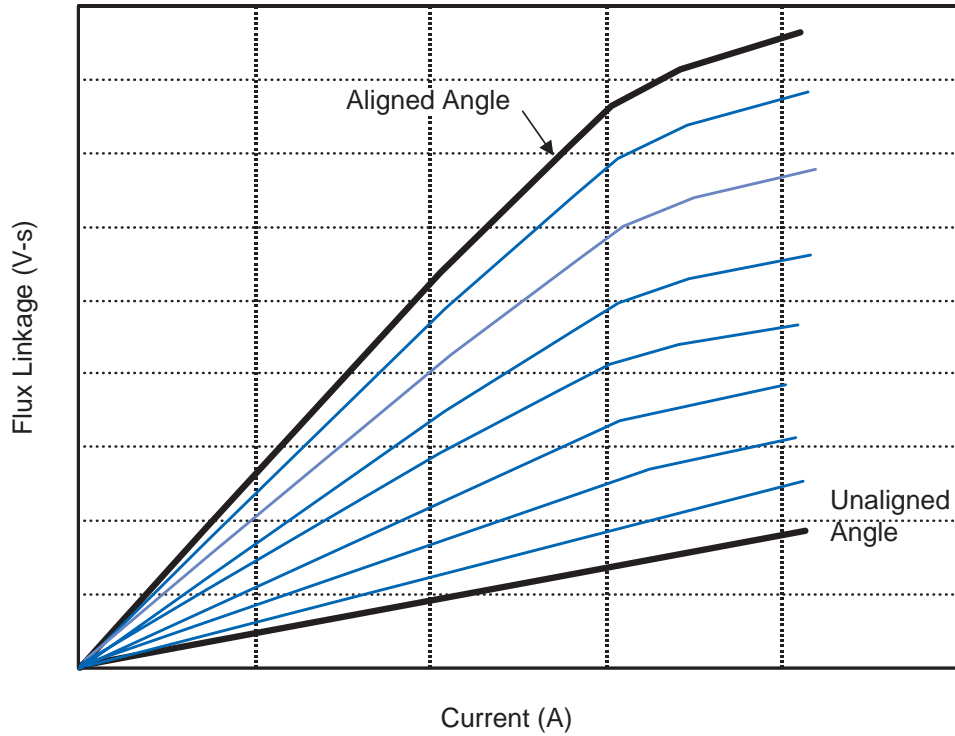
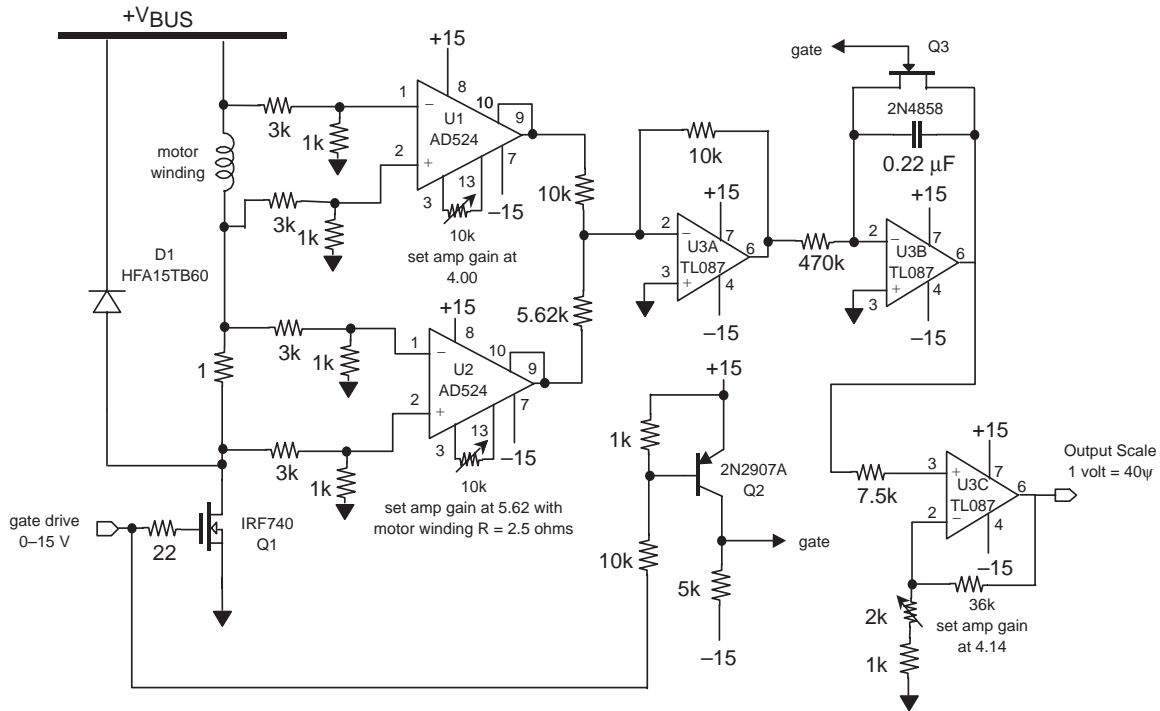


Figure 17. SRM Magnetization Curves

### 3.5.1 Flux Measurement Hardware

Figure 18 shows the schematic of the analog flux measurement hardware used to collect magnetic data for the SRM used in the demonstration platform. In the SRM, flux linkage in each phase of the motor can be calculated from the basic equation  $\hat{\lambda} = \int (V - iR) dt$ , relating flux linkage ( $\hat{\lambda}$ ) to voltage across the phase winding and current flow through the winding. Referring to the schematic, the semiconductor switch (Q1) controls the current through the SRM phase winding and is driven by a pulse generator at the gate drive input with a pulse width that is adjusted to allow the current to reach a steady-state level. For the SRM used in this demonstration platform with an electrical time constant of 20 msec, the pulse width of the gate drive should be set to approximately 100 msec.



**Figure 18. Analog Flux Measurement Circuit**

The voltage level at  $+V_{BUS}$  should be adjusted for the maximum current desired for the flux measurement. Due to limitations in the measurement circuitry, the  $+V_{BUS}$  should never be set greater than about +40 volts dc. Differential instrumentation op amps (U1 and U2) measure the voltage across the phase winding and the current flow through the winding with a current-sensing resistor of 1 ohm. The summation amplifier (U3A) subtracts the  $i r_W$  drop from the voltage across the winding to  $v - i r_W$  form and the result is then integrated in the reset integrator (U3B) to form the flux measurement ( $\hat{\lambda}$ ). Gains shown in the schematic have been set to give reasonable values within the dynamic range of the circuitry for the SRM used in this demonstration platform. Other SRMs may require different scaling to give correct results of flux measurement.

### 3.5.2 Demo SRM Flux Measurements

Magnetization flux data was collected on the SRM used in the demonstration platform from low current levels to a maximum current of 4 amps. Figure 19 shows this flux linkage data over this current range at the aligned rotor position. Note that the curve is very linear to the maximum current level of 4 amps, indicating no magnetic saturation at these current levels. Also, the slope of the curve as measured is the inductance of the SRM at the aligned position and indicates an inductance of about 52 mH. Flux linkage data from measurements of all three phases of the SRM are shown and indicate excellent balance between the phase windings for this particular SRM.

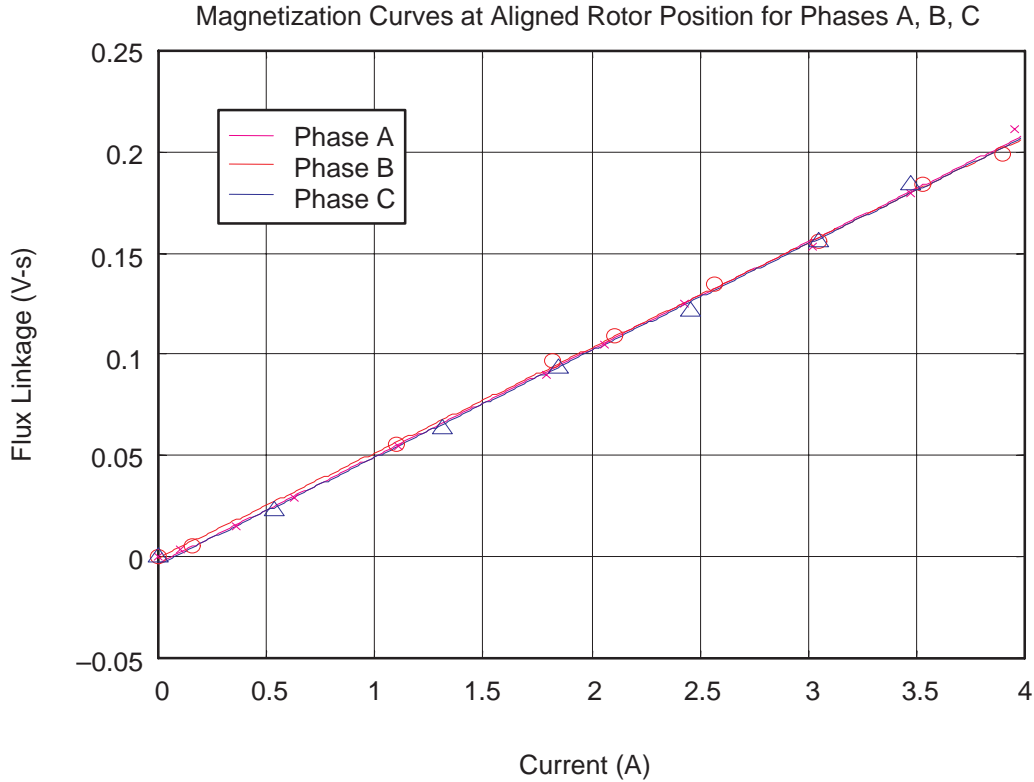


Figure 19. Flux Linkage Curves for Demo Platform SRM

### 3.5.3 Look-up Table Generation Method

To generate a look-up table from the raw magnetization data, a polynomial curve fit is performed on the data. For the motor used in the demonstration, the magnetization curve is very linear up to the maximum operating current of 4.0 A, and a first-order curve accurately fits the data. However, other motors may have magnetization curves which are nonlinear, and a higher-order polynomial may be needed to capture the “knee” of the curve. After the fitting, the function is evaluated at the currents

$$i_n = i_{\max} \left( \frac{n}{256} \right) \quad \forall n = 0 \dots 255 \quad (17)$$

These points are chosen to allow an index into the 256-point look-up table to be calculated by right-shifting the 10-bit current measurement over two places. After generating the look-up table, it is multiplied by the scaling factor  $n_{\max} f_s$  (maximum duty cycle count times the sampling frequency) to make it compatible with the scaling of the flux estimator. The reasons for this particular flux scaling are discussed in Section 2.

## References

1. Lyons, J., S. MacMinn, and M. Preston. "Flux/Current Methods for SRM Rotor Position Estimation." IEEE IAS Meeting Conf. Record, 1991.

## **IMPORTANT NOTICE**

Texas Instruments and its subsidiaries (TI) reserve the right to make changes to their products or to discontinue any product or service without notice, and advise customers to obtain the latest version of relevant information to verify, before placing orders, that information being relied on is current and complete. All products are sold subject to the terms and conditions of sale supplied at the time of order acknowledgement, including those pertaining to warranty, patent infringement, and limitation of liability.

TI warrants performance of its semiconductor products to the specifications applicable at the time of sale in accordance with TI's standard warranty. Testing and other quality control techniques are utilized to the extent TI deems necessary to support this warranty. Specific testing of all parameters of each device is not necessarily performed, except those mandated by government requirements.

**CERTAIN APPLICATIONS USING SEMICONDUCTOR PRODUCTS MAY INVOLVE POTENTIAL RISKS OF DEATH, PERSONAL INJURY, OR SEVERE PROPERTY OR ENVIRONMENTAL DAMAGE ("CRITICAL APPLICATIONS"). TI SEMICONDUCTOR PRODUCTS ARE NOT DESIGNED, AUTHORIZED, OR WARRANTED TO BE SUITABLE FOR USE IN LIFE-SUPPORT DEVICES OR SYSTEMS OR OTHER CRITICAL APPLICATIONS. INCLUSION OF TI PRODUCTS IN SUCH APPLICATIONS IS UNDERSTOOD TO BE FULLY AT THE CUSTOMER'S RISK.**

In order to minimize risks associated with the customer's applications, adequate design and operating safeguards must be provided by the customer to minimize inherent or procedural hazards.

TI assumes no liability for applications assistance or customer product design. TI does not warrant or represent that any license, either express or implied, is granted under any patent right, copyright, mask work right, or other intellectual property right of TI covering or relating to any combination, machine, or process in which such semiconductor products or services might be or are used. TI's publication of information regarding any third party's products or services does not constitute TI's approval, warranty or endorsement thereof.